J Fluoresc (2012) 22:1475–1482
DOI 10.1007/s10895-012-1084-7

ORIGINAL PAPER

Fluorescence Characteristics of Isolated Dye Molecules within Silicalite-1 Channels

Tae Kyu Shim · Myoung Hee Lee · Doseok Kim · Hyun Sung Kim · Kyung Byung Yoon

Received: 9 January 2012 / Accepted: 20 June 2012 / Published online: 28 June 2012

Abstract Fluorescence characteristics of hemicyanine dye molecules isolated from neighboring molecules and strongly restricted inside nanosized pores of zeolite (silicalite-1) crystal were investigated. For samples in which the molecules were sufficiently far away from the others, the fluorescence decay lifetime of the molecules was about 2.2 ns. As the intermolecular distance was reduced, the steady-state fluorescence peak shifted toward the longer wavelength and the fluorescence efficiency decreased markedly. The fluorescence decay lifetime also decreased to 0.8 ns for a sample with the smallest intermolecular distance of 2.1 nm. These results were explained in terms of a dipole-dipole interaction between pairs of dye molecules. From the relation between the intermolecular distances and the fluorescence decay lifetimes of the molecules, the radius of energy transfer of hemicyanine donor-acceptor pair in zeolite matrix was determined to be 2.2 nm, in fair agreement with the calculated Förster radius between dye molecules of the same species.

Keywords Fluorescence · Hemicyanine · Silicalite-1 · Foerster energy transfer · FRET

Introduction

As a host material of organic molecules or inorganic complexes, zeolite has many advantages by providing environment of uniform nano-sized pores or channels of well-defined size, which makes it attractive to investigate photophysical properties of the materials enclosed in such environment [1–5]. Förster energy transfer [6–9] of dye molecules enclosed in zeolite pores or channels has been studied for possible applications as artificial light-harvesting system [1, 10–12]. Lasing action from dye molecules inserted in zeolite has been reported [13, 14]. Zeolite crystals were self-assembled on a glass plate with their vertical channels well-oriented normal to the surface, which allowed the macroscopic, unidirectional alignment of inserted nonlinear optical molecules for optical second-harmonic generation [3, 15–17].

As one of the key photophysical characteristics, the radiative properties of organic molecules or inorganic nanocomplexes in the nano-confined environment can also be an interesting subject [11, 12, 18, 19]. Especially, confinement of fluorescent dye molecules in such environments has been known to change their radiative efficiency drastically. The underlying mechanisms are very diverse as cavity quantum-electrodynamic effect (atomic system in a cavity [20], semiconductor quantum dot in a Bragg-reflector [21]), change of electric field strength (dye molecule or dye complex near the metallic surface [22–24]), radiative energy transfer (between nearby dye molecules [24, 25]), and inhibition of intramolecular rotation (dye molecules in zeolite with narrow pores or channels [5]).

Among the processes listed above, energy transfer between dye molecules is a phenomenon of fundamental importance, and has found widespread applications in single-molecule biophysics [26–30]. This fluorescence resonant energy transfer (FRET) has been studied mostly between a pair consisting of two different dye molecules commonly called a donor and an acceptor. The underlying theory developed by Förster [6, 7] can equally be applied to the energy transfer between dye molecules of the same kind, and there have been several studies on this *homo-FRET*

T. K. Shim · M. H. Lee · D. Kim (✉)
Department of Physics, Sogang University,
Seoul 121-742, South Korea
e-mail: doseok@sogang.ac.kr

H. S. Kim · K. B. Yoon
Center for Microcrystal Assembly, Department of Chemistry,
and Program of Integrated Biotechnology, Sogang University,
Seoul 121-742, South Korea

process [31–34], which studied the rate of the intermolecular energy migration between dye molecules in solution or between fluorescent protein labels [33, 34]. There are some issues on this phenomenon that awaits more systematic study. For example, Förster radius (a characteristic length scale over which the total decay rate of the donor molecule doubles from that of an isolated dye molecule) between the same dyes could be investigated systematically by changing the distance between dye molecules. Physical overlap between the fluorophores and the resulting change in the electronic structure has been considered to cause fluorescence quenching. However, it hasn't been easy to control the situation that relates to fluorescence quenching, as dyes usually form an aggregate if one tried to decrease the inter-dye distance by increasing the concentration in a solution. Regarding the issue, it might be useful to understand the fluorescence characteristics of dye molecules with controlled intermolecular distances, which would provide insights for fundamental understanding of the phenomenon.

In this work, we prepared hemicyanine dye molecules inserted in silicalite-1 with varying intermolecular distances, and measured their steady-state and time-resolved fluorescence properties. Fluorescence quenching phenomenon and redshift of the fluorescence peak were observed by decreasing the intermolecular distance between dye molecules of the same kind enclosed in silicalite-1 channels. These phenomena suggested that the energy transfer between molecules and the accompanying fluorescence decay lifetime change could be explained well in terms of the Förster energy transfer mechanism.

Materials and Methods

Materials

The dye molecule used for this study is hemicyanine (4-[4-(dimethylamino) styryl]-1-n-alkylpyridinium bromide, hereafter denoted HC-n). The alkyl chain length used was usually 3 (HC-3), and we used HC-18 to check for the possibility of Dexter-type energy transfer mechanism [35].

Figure 1a shows the chemical structure of the hemicyanine molecule. The insertion of hemicyanine molecules in silicalite-1 has been described in previous report [3]. The size of the silicalite-1 crystal used is 400 nm as in our previous report [3]. The adsorption site of these silicalite-1 crystals is their straight channels with the channel diameter of 5.5 Å (Fig. 1a), which is similar to the lateral size of the HC-n molecule such that the adsorbed dye would hardly move inside. Moreover the HC-n molecules are adsorbed only along this vertical channel, as the interconnecting side channels are bent and not likely to accept 1~2 nm-long hemicyanine molecules [16, 36–38]. Figure 1a shows the

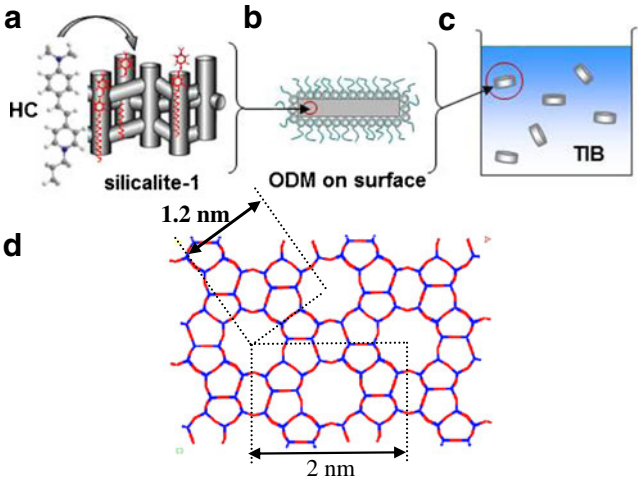

Fig. 1 **a** Molecular structure of hemicyanine dye used in this work and silicalite-1 structure loaded with dyes along the straight channels. **b** ODM (octadecyltrimethoxysilane) treated silicalite-1 crystal. **c** Well-dispersed silicalite-1 crystal loaded with dyes in TIB (triisopropylbenzene) solvent. **d** Structure of the silicalite-1 crystal showing distances between the nearest- and the next-nearest vertical channels

schematic of the hemicyanine molecules adsorbed along the vertical channels of the silicalite-1. The accurate determination of the number density of included hemicyanine molecule (hence the intermolecular distance) in silicalite-1 was crucial for this study, and the method to get this value was described in earlier report [3]. In brief, the silicalite-1 containing HC-n made by the same condition as the ones in the optical measurement was completely dissolved in hydrofluoric acid, and the extinction coefficient from the resulting solution was measured to determine exact amount of incorporated dye molecules. As the distribution of the molecules is believed to be homogeneous across the volume of the silicalite-1 crystal [3], the intermolecular distance was simply estimated to be $N^{-1/3}$, where N is the number density of the adsorbed molecules [39]. As shown in Fig. 1b, these silicalite-1 crystals with known number-density of incorporated dyes were then capped with octadecyltrimethoxysilane (ODM) molecules, and dispersed into triisopropylbenzene (TIB) solvent for fluorescence measurement like in Fig. 1c. The ODM capping was used to keep the incorporated dye from spilling out of the silicalite-1 channel, and triisopropylbenzene (TIB) molecule is chosen as it is large enough and round in shape and cannot enter into the silicalite-1 channel (SI.4). Also its refractive index is very close to that of silicalite-1 such that it can minimize the effect of scattering from silicalite-1 crystals. These preparations were in fact not critical as the measurement on HC-n/silicalite-1 crystals (not surface treated) just piled up in air gave nearly the same result. Figure 1d shows the distances between the nearest- and the next-nearest vertical channels in which the dyes are adsorbed.

Spectroscopic Measurements

Steady-state absorption spectra were deduced by measuring the reflection from the HC-n/silicalite-1 sample, and the steady-state fluorescence was measured by the standard method. To measure the time-resolved fluorescence from the HC-n/silicalite-1 sample (HC-n/silicalite-1 powder or HC-n/silicalite-1 dispersed in TIB solvent), a second-harmonic of the femtosecond Ti:sapphire laser (800 nm, 100 fs pulsewidth, 82 MHz repetition rate) output was used as an excitation source. The pump energy was kept below 0.5 mW, and with this pump energy, only ~2 % of the dye molecules in silicalite-1 are estimated to be in the excited state for the sample with medium dye loading. Thus a donor dye (in excited state) is most likely to be near an acceptor dye (in ground state), and 'excimer formation' or interaction between dye in excited state cannot happen with the above experimental condition. Changing the pump intensity by about an order did not change the observed phenomenon either. The collected fluorescence signal from HC-3/silicalite-1 was dispersed by using a monochromator to have 2-nm resolution and detected by using a fast photomultiplier tube and a photon counting system (SPC730, Becker & Hickl) for time-correlated single-photon counting (TCSPC). The instrument response function (IRF) from the detection electronics has FWHM of 150 ps, which was deconvolved using the commercial fitting software (Picoquant, FluoFit). All the spectra were measured at room temperature.

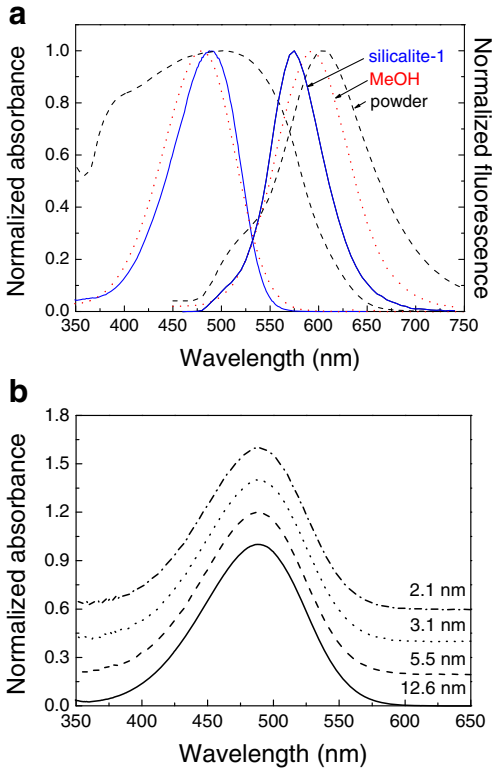

Fig. 2 **a** Steady-state absorption and fluorescence spectra of hemicyanine in methanol (1×10^{-5} M, solid lines), in the silicalite-1 (*dotted lines*), and in molecular crystalline, powder form (*dashed lines*). **b** The absorption spectra for HC-3/silicalite-1, intermolecular distance—12.6 nm (*solid line*), 5.5 nm (*dashed line*), 3.1 nm (*dotted line*), and 2.1 nm (*dash dotted line*). The spectra were shifted upwards for clarity

Results and Discussion

Figure 2a shows the steady-state absorption and the fluorescence spectra of the samples in different environments. As shown in this figure, the Stokes shift of the dye in silicalite-1 is less than that in methanol solvent, which would reflect the differences in dielectric and solvation properties of the two different surrounding media [5]. The absorption and fluorescence spectra of the HC-3 in pure crystalline powderform were qualitatively very different (with wider bandwidths and shoulders around the peak) from those in methanol and in silicalite-1, indicating that the stronger intermolecular interaction altered the electronic structure of the molecules as compared to those in isolation. By contrast, the absorption spectra in Fig. 2b remained the same throughout the concentration range we investigated, ensuring that even at the highest concentration the dye molecules in silicalite-1 matrix exist as a monomer, well isolated by the channel walls without forming molecular aggregates.

From Fig. 3, on the other hand, the redshift of the fluorescence peak and reduction of fluorescence efficiency with decreased intermolecular distance are easily noticeable. The initial fluorescence peak at 570 nm (for an intermolecular distance of 12.6 nm) redshifts by as much as~45 nm for a sample with the shortest intermolecular distance of 2.1 nm, concurrently with reduced fluorescence intensity. The reabsorption of the fluorescence is not responsible as the sample with much smaller concentration of dispersed HC-3/silicalite-1 crystals showed essentially the same fluorescence

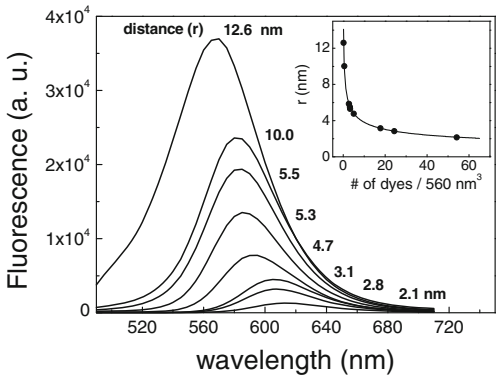

Fig. 3 Variations of the steady-state fluorescence of hemicyanine in the silicalite-1 with varying dye concentration. The numbers beside the fluorescence spectra indicate the intermolecular distance. The inset shows the intermolecular distances of the samples used in the experiments using $N^{1/3}$

spectra. This result also indicates that the dye-in-silicalite-1 system is very different from more usual HC-n solution, where the peak shape and the fluorescence quantum yield do not change appreciably even at the highest concentration achievable before the molecules form aggregates.

To account for the interesting behavior shown in Fig. 3, intermolecular dipole-dipole interaction (Förster energy transfer) between the dye molecules was proposed for responsible mechanism. Förster energy transfer requires excited donor molecule and the acceptor molecule of which the absorption band overlaps with the fluorescence spectrum of the donor molecule. This is usually achieved with two different dye molecules (donor and acceptor) chosen for maximal spectral overlap, and is widely used in biology and chemistry as a nanoscale ruler [29, 40]. In this experiment, the pair of hemicyanine molecules (one in excited state and the other in ground state) would work as a donor and an acceptor molecule, utilizing the overlap of absorption and fluorescence spectra of hemicyanine in silicalite-1 (solid lines in Fig. 2a). As the distance r between the molecules is getting closer, the rate of energy transfer from donor to acceptor molecule by dipole-dipole interaction would increase steeply as r^{-6}. The redshift of fluorescence peak can be explained as the acceptor molecule can only emit at lower energies than the energy of donor-acceptor spectral overlap, eating up the blue-part of the fluorescence spectra and causing the overall redshift of the fluorescence spectra.

To check for the possibility of energy relaxation by different mechanism, two samples heavily loaded with HC-3 and HC-18 with the same number density of dyes were prepared to control the possible overlap of wavefunctions of closest molecules (Dexter process). Even with much longer alkyl chain at one end to allow different degree of possible spatial overlap of the core wavefunctions between nearby molecules, the fluorescence spectrum and the fluorescence decay lifetime for HC-18 were very similar to those of HC-3 even for the samples with shortest intramolecular distance, confirming the Dexter-type energy transfer can be ruled out for the relaxation mechanism in our system [35].

This environment of dye molecules in small channels of the silicalite-1 is very different from the environment in which the molecules are forming a molecular crystal. In the latter case the proximity of the neighboring molecules introduces various midgap states and nonradiative decay channels and changes the steady-state absorption and fluorescence spectra markedly as in the dashed lines in Fig. 2, such that the crystallized molecules lose the photophysical properties of the single molecule. The introduction of nonradiative decay channels is also evident from the much faster fluorescence decay of hemicyanine powder in Fig. 4b. These observations demonstrate that the silicalite-1 matrix provides an *ideal framework* to study the radiative

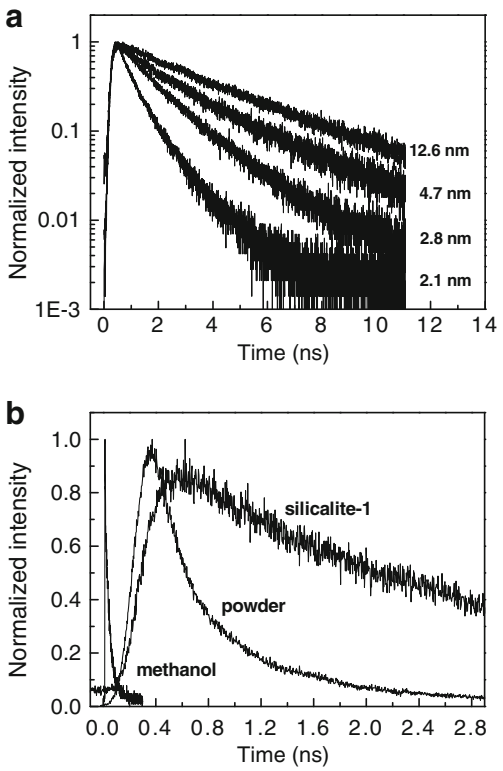

Fig. 4 **a** Fluorescence decay curves of hemicyanine in the silicalite-1 with increasing concentration of dye (The intermolecular distances are 2.1, 2.8, 4.7, and 12.6 nm, respectively). **b** Fluorescence decay curves of hemicyanine in methanol solution, in the silicalite-1, and in powder form. Fluorescence in methanol was obtained using upcoversion method (time resolution ~300 fs), and the other fluorescence data were obtained using TCSPC (instrument response function ~150 ps)

properties of a dye molecule and make it possible to isolate molecules even at very small intermolecular distance *unachievable in solution phase* while hardly perturbing the electronic structure of the molecule.

For confirmation of the proposed mechanism and more quantitative analysis, we investigated the fluorescence dynamics of the dyes with different intermolecular distances by using TCSPC method [41]. Figure 4a indicates the fluorescence decay curves of the samples with varying dye concentrations measured at 570 nm, peak position of fluorescence corresponding to the sample of the lowest concentration. The fluorescence decay for the sample with the lowest concentration can be fitted well with single exponential with the lifetime of 2.2 ns. As the dye concentration in silicalite-1 matrix increased, the fluorescence decayed significantly faster. Furthermore, for highly loaded samples, two exponential components were necessary to fit the fluorescence decay curve, which means that the relaxation of the dyes in excited state is through several independent deactivation pathways. To compare the fluorescence decays at different concentrations quantitatively, the fluorescence decay curves are fitted with two-exponential function $A_1 \exp$

$(-t/\tau_1)+A_2\exp(-t/\tau_2)$, and the average fluorescence decay lifetime is defined in usual way as $\tau_{ave}=(A_1\tau_1+A_2/\tau_2)/(A_1+A_2)$. With the above analysis, average fluorescence decay lifetime for the highest loaded sample shortened significantly to 800 ps.

Calzaferri and co-workers reported that the energy transfer between two different dye molecules (donor and acceptor) randomly mixed in zeolite-L changes with the dye concentration [42–44]. In their data that showed fluorescence decay of acceptors (oxonine dyes), one of the terms in the multi-exponential fitting had negative prefactor ($A_1<0$, accounting for slow rise of fluorescence after the laser pulse), which means that the acceptors are excited by means of energy transfer from the donor molecules. By contrast, in our case, the fitted result did not show any negative prefactor. This indicates we selectively probed the dye molecules in the ensemble that worked as donors by monitoring blue-edge of the fluorescence spectra. Thus the fluorescence decay results are analyzed in the following in terms of the energy transfer of the donor molecules.

The variation of the average fluorescence decay lifetime with increasing intramolecular distance is shown in Fig. 5, where the decay lifetimes were obtained from two-exponential fitting of the curves in Fig. 4 and $\tau_{ave}=(A_1\tau_1+A_2/\tau_2)/(A_1+A_2)$. From this result, we can obtain the energy transfer radius (γ_0, Förster radius), for which the dipole-dipole energy transfer rate equals the fluorescence decay rate without any acceptor molecules (termed intrinsic decay rate from now on) [6–8]. The measured decay rate $\kappa=1/\tau_{ave}$ of excited dye molecule can be expressed as

$$k = k_0 + k_{nr} \tag{1}$$

where κ_0 and κ_{nr} are the intrinsic radiative and nonradiative decay rates of the chromophore, respectively. The rate of Förster energy transfer (κ_{ET}) between donor and acceptor depends on the intermolecular distance r and the mutual orientation between the donor and the acceptor molecules as [7–9],

$$k_{ET} = \frac{3}{2}\left\langle k^2\right\rangle \frac{1}{\tau_D}\left(\frac{r_0}{r}\right)^6$$
$$with\left\langle k^2\right\rangle = \frac{1}{4\pi}\int_0^{2\pi}\int_0^{\pi} k^2 \sin\theta d\theta d\phi \tag{2}$$

where $\tau_D=1/k_0$ is the intrinsic decay lifetime of the single donor molecule in silicalite-1 channel without acceptors, and κ^2 is an orientational factor. The orientational factor is given by $\kappa^2=(\cos\theta_T-3\cos\theta_D\cos\theta_A)^2$, where θ_T is the angle between donor and acceptor transition dipole moment, θ_D and θ_A and are angles between line connecting the center of donor and acceptor and the donor and the acceptor transition dipole moments, respectively [45, 46]. When the molecular orientation is much faster than the energy transfer (i.e. the case of dynamic averaging), the orientational factor is $<\kappa^2>=2/3$. However, in our system, all the molecules are aligned along the vertical channel, and the dipole directions are the same between the donor and acceptor molecules ($\theta_D=\theta_A$). Thus by setting $\theta_D=\theta_A=\theta$ and $\theta_T=0$ in the expression $\kappa^2=(\cos\theta_T-3\cos\theta_D\cos\theta_A)^2$ and averaging over all directions (the energy transfer is expected to happen between fluorophores in the same channel and in neighboring channels equally well) by using Eq. (2), the orientational factor in our case is $<\kappa_{nr}>=4/5$ [45].

By assuming Förster energy transfer is responsible for observed lifetime change, $\kappa_{ET}=\kappa_{nr}$, the measured decay lifetime is described as below from the Eqs. (1) and (2).

$$\tau_{ave} = \frac{1}{k} = \frac{\tau_D}{1+\frac{6}{5}\left(\frac{r_0}{r}\right)^6} \tag{3}$$

By fitting the data in Fig. 5 using the above relation, we could determine the Förster radius (r_0=2.2 nm) and donor decay lifetime (τ_D=2.2 ns) of hemicyanine dye in silicalite-1 matrix. In Fig. 5, the fluorescence decay lifetimes could be obtained for intermolecular distances ranging from r= 12.6 nm to 2.1 nm. This smooth change of intermolecular distance across Förster radius is only possible due to silicalite-1 matrix, providing rigid and inert channel walls to isolate the molecules without disturbing their electronic structures. In contrast, the highest concentration of hemicyanine solution without forming an aggregate was about ~0.01 mol/L, where intermolecular distance was still 5.5 nm. As this distance is appreciably larger than the Förster radius, the radiative properties did not change appreciably from normal diluted solutions.

Using two-exponential function to fit the decay curve is only heuristic (to estimate τ_{ave}), and the fluorescence decay

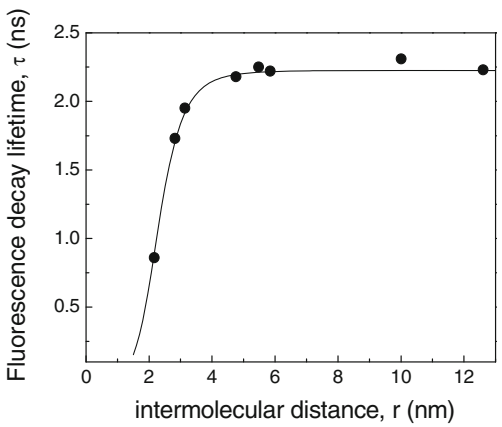

Fig. 5 Average decay lifetimes of the samples vs. intermolecular distance, *Solid line* is the fitted result using Eq. (3)

under dipole-dipole interaction is usually fitted using a non-exponential function as below [8, 44, 47, 48].

$$I(t) = \exp\left[-\frac{t}{\tau_D} - \sqrt{\frac{16\pi^3\langle k^2\rangle t}{18\tau_D}} n_A {r_0}^3\right] = \exp\left[-\frac{t}{\tau_D} - \sqrt{\frac{t}{\tau_D}} A\right], \quad \text{where } A = \sqrt{\frac{16\pi^3\langle k^2\rangle}{18}} n_A {r_0}^3 \tag{4}$$

where τ_D is the decay lifetime of dye molecule without any surrounding molecules, $<\kappa^2>$is the same orientational factor as in Eq. (2) and n_A is the number density of the molecules. This equation was devised to describe radiative properties of the ensemble of dyes with the concentration change in the system [8, 44, 47, 48]. With τ_D=2.2 ns from the fluorescence decay measurement with much diluted sample, we fitted the fluorescence decay curves for samples of different loading densities. As all the factors in the above equation except r_0 are known, the Förster radius r_0 should be deduced from the fitting of the fluorescence decay curves. From the results obtained from the non-exponential model, we found the Förster radius of the molecules in silicalite-1 matrix is about 1.9 nm. This r_0 value is in fair agreement with the value obtained from the experiment using Eq. (3), and remarkably well, remained the same for fluorescence decay curves of all the samples having different dye concentrations as measured in this study.

The Förster radius can be calculated from the spectral properties of donor and acceptor and the fluorescence quantum yield of the donor as follow [7–9],

$$r_0 = 0.211\left[\langle k^2\rangle n^{-4} Q_D J(\lambda)\right]^{1/6} \tag{5}$$

where Q_D is the quantum yield of the donor, $<\kappa^2>$is the same orientational factor as in Eq. (2) [7, 9], n=1.4 is the refractive index of the medium, and $J(\lambda)$ is the spectral overlap integral of the fluorescence spectrum of donor and the absorption spectrum of acceptor. The fluorescence quantum yield of the donor (HC-3) molecule in silicalite-1 channel is estimated to be 0.3 from the previous reports [49, 50]. From these values, the theoretical Förster radius of the hemicyanine molecule donor-acceptor pair is about 2.1 nm, in fair agreement with the value obtained from the experiment.

Finally, observed phenomenon of decrease in fluorescence quantum yield with the decrease in intermolecular distance can be related to fluorescence quenching. Even if fluorescence quenching has been known for decades, our understanding is far from complete as it is observed in various systems with diverse characteristics [9, 38, 46, 51–53]. It is because the increase in nonradiative decay rate responsible for fluorescence quenching can be caused by various origins such as excited state reactions, complex formation, wavefunction overlap, and energy transfer [8, 9, 54]. It has also been commonly supposed that physical overlap between dye molecules is essential for fluorescence quenching. In the current case of HC-n/silicalite-1 system, presence of silicalite-1 matrix allows us to exclude dye aggregation, wavefunction overlap, and complex formation as mechanisms for fluorescence quenching. Thus, fluorescence quenching in this system could be explained well in terms of the Förster energy transfer mechanism.

Conclusions

In conclusion, fluorescence characteristics of hemicyanine dye molecules isolated in silicalite-1 with nano-sized channels were investigated, and the dipole-dipole interaction between molecules were proposed to explain the observed phenomenon. To quantitatively estimate the critical distance of energy transfer (Förster radius), we varied the distance between molecules using different concentrations of the dyes in the silicalite-1 channels. For the molecules with intermolecular distance above ~5 nm, the decay lifetime reached a value of 2.2 ns, which can be attributed to the fluorescence dynamics of the single molecule well isolated in the silicalite-1 nanochannels. However, for the molecules having shorter intermolecular distances, the decay lifetime shortened significantly to ~800 ps. From the relation between the measured decay lifetimes and the intermolecular distances, the Förster radius of the hemicyanine dye in silicalite-1 nanochannels was determined, which is in good agreement with the value estimated from the theory that took into account the characteristics of the molecule including the spectral overlap.

Acknowledgments This work was supported by the Korean Government (MEST) grant No. 2011-0017435, SRF grant (201214003) of the Sogang University, and by the Korea Center for Artificial Photosynthesis located in Sogang University funded by MEST through the National Research Foundation of Korea (NRF-2009-C1AAA001-2009-0093879).

References

1. Calzaferri G, Huber S, Maas H, Minkowski C (2003) Host–guest antenna materials. Angew Chem Int Ed 42(32):3732–3758
2. Nguyen T, Wu J, Doan V, Schwartz BJ, Tolbert SH (2000) Control of energy transfer in oriented conjugated polymer-mesoporous silica composites. Science 288(5466):652–656
3. Kim HS, Lee S, Ha K, Jung C, Lee Y, Chun Y, Kim D, Rhee BK, Yoon KB (2004) Aligned inclusion of hemicyanine dyes into silica zeolite films for second harmonic generation. J Am Chem Soc 126 (2):673–682
4. Macchi G, Botta C, Calzaferri G, Catti M, Cornil J, Gierschner J, Meinardi F, Tubino R (2010) Weak forces at work in dye-loaded zeolite materials: spectroscopic investigation on cation–sulfur interactions. Phys Chem Chem Phys 12(11):2599–2605

5. Shim TK, Lee MH, Kim D, Kim HS, Yoon KB (2009) Fluorescence properties of hemicyanine in the nanoporous materials with varying pore sizes. J Phys Chem B 113(4):966–969
6. Förster Th (1948) Intermolecular energy migration and fluorescence. Ann Phys (Leipzig) 2(6):55–75
7. Andrews DL, Demidov AA (1999) Resonance energy transfer. John Wiley & Sons, England, pp 151–172
8. Valeur B (2002) Molecular fluorescence: principles and applications. Wiley-VCH, Weinheim, Germany, pp 247–272
9. Lakowicz JR (2006) Principles of Fluorescence Spectroscopy, 3rd edn. Springer, New York, pp 443–475
10. Calzaferri G, Lutkouskaya K (2008) Mimicking the antenna system of green plants. Photochem Photobiol Sci 7(8):879–910
11. Busby M, Blum C, Tibben M, Fibikar S, Calzaferri G, Subramaniam V, Cola LD (2008) Time, space, and spectrally resolved studies on J-aggregate interactions in zeolite L nanochannels. J Am Chem Soc 130(33):10970–10976
12. Vohra V, Devaux A, Dieu LQ, Scavia G, Catellani M, Calzaferri G, Botta C (2009) Energy transfer in fluorescent nanofibers embedding dye-loaded zeolite L crystals. Adv Mater 21(10–11):1146–1150
13. Vietze U, Krass O, Laeri F, Ihlein G, Schueth F, Limburg B, Abraham M (1998) Zeolite-dye microlasers. Phys Rev Lett 81 (21):4628–4631
14. Li IL, Tang ZK, Xiao XD, Yang CL, Ge WK (2003) Optical properties of organic dyes in nanoporous zeolite crystals. Appl Phys Lett 83(12):2438–2441
15. Cox SD, Gier TE, Stucky GD, Bierlein J (1988) Inclusion tuning of nonlinear optical materials: switching the SHG of p-nitroaniline and 2-methyl-p-nitroaniline with molecular sieve hosts. J Am Chem Soc 110(9):2986–2987
16. Gao F, Zhu G, Chen Y, Qiu S (2004) Assembly of p-nitroaniline molecule in the channel of zeolite MFI large single crystal for NLO material. J Phys Chem B 108(11):3426–3430
17. Shim TK, Kim D, Lee MH, Rhee BK, Cheong HM, Kim HS, Yoon KB (2006) Determination of the hyperpolarizability components of hemicyanine dyes by measuring the anisotropic fluorescence and second harmonic of the dyes uniformly aligned within zeolite channels. J Phys Chem B 110(34):16874–16878
18. Szulbinski WS, Ma'nuel DJ, Kincaid JR (2001) Zeolite-entrapped organized molecular assemblies. New evidence for highly efficient adjacent cage dyad formation and constrained rotational mobility of tris-Ligated polypyridine complexes. Inorg Chem 40(14):3443–3447
19. Hashimoto S, Moon HR, Yoon KB (2007) Optical microscopy study of zeolite-dye composite materials. Microporous Mesoporous Mater 101(1–2):10–18
20. Hinds EA (1990) Cavity quantum electrod dynamics. Adv At Mol Opt Phys 2:237–289
21. Solomon GS, Pelton M, Yamamoto Y (2001) Single-mode spontaneous emission from a single quantum dot in a three-dimensional microcavity. Phys Rev Lett 86(17):3903–3906
22. Chance RR, Prock A, Silbey R (1978) Molecular fluorescence and energy transfer near interfaces. Adv Chem Phys 37:1–65
23. Andrews P, Barnes WL (2004) Energy transfer across a metal film mediated by surface plasmon polaritons. Science 306(5698):1002–1005
24. Lakowicz JR (2001) Radiative decay engineering: biophysical and biomedical applications. Anal Biochem 298(1):1–24
25. Ali M, Ahmed SA, Kitwally K (1989) Fluorescence and gain predictions in laser dye mixtures. Appl Opt 28(17):3708–3712
26. Schuler B, Lipman EA, Eaton WA (2002) Probing the free-energy surface for protein folding with single-molecule fluorescence spectroscopy. Nature 419(6908):743–747
27. Michalet X, Kapanidis AN, Laurence T, Pinaud F, Doose S, Pflughoefft M, Weiss S (2003) The power and prospects of fluorescence microscopies and spectroscopies. Annu Rev Biophys Biomol Struct 32:161–182
28. Kajihara D, Abe R, Iijima I, Koiyama C, Sisido M, Hohsaka T (2006) FRET analysis of protein conformational change through position-specific incorporation of fluorescent amino acids. Nat Methods 3:923–929
29. Joo C, Balci H, Ishitsuka Y, Buranachai C, Ha T (2008) Advances in single-molecule fluorescence methods for molecular biology. Annu Rev Biochem 77:51–76
30. Borgia A, Williams PM, Clarke J (2008) Single-molecule studies of protein folding. Annu Rev Biochem 77:101–125
31. Weber G (1954) Dependence of the polarization of the fluorescence on the concentration. Trans Faraday Soc 50:552–555
32. Johnson ID, Kang HC, Haugland RP (1991) Fluorescent membrane probes incorporating dipyrromethemeboron difluoride fluorophores. Anal Biochem 198(2):228–237
33. Patterson GH, Piston DW, Barisas BG (2000) Förster distances between green fluorescent protein pairs. Anal Biochem 284 (2):438–440
34. Isaksson M, Kalinin S, Lobov S, Wang S, Nyb T, Johansson LB (2004) Partial donor–donor energy migration (PDDEM): a novel fluorescence method for internal protein distance measurements. Phys Chem Chem Phys 6(11):3001–3008
35. Turro NJ (1991) Modern Molecular Photochemistry. University Science, Mill Valley, pp 305–311
36. Schuth F (1992) Polarized fourier transform infrared microscopy as a tool for structural analysis of adsorbates in molecular sieves. J Phys Chem 96(19):7493–7496
37. Kox MHF, Stavitski E, Weckhuysen BM (2007) Nonuniform catalytic behavior of zeolite crystals as revealed by in situ optical microspectroscopy. Angew Chem Int Ed 46(20):3652–3655
38. Karwacki L et al (2009) Morphology-dependent zeolite intergrowth structures leading to distinct internal and outer-surface molecular diffusion barriers. Nat Mater 8:959–965
39. Assuming a random distribution of molecules in zeolite, *statistically* the dyes can be closer than $N^{-1/3}$ by as much as 0.554 (Chandrasekhar S (1943) Stochastic problems in physics and astronomy. Rev Mod Phys 15(1):1–89). This aspect has not been taken into account in our ensemble-averaged measurements, but can be used in more elaborate analysis especially when one considers that the dyes closer together would transfer energy much more efficiently
40. Schuler B, Lipman EA, Steinbach PJ, Kumke M, Eaton WA (2005) Polyproline and the "spectroscopic ruler" revisited with single-molecule fluorescence. Proc Natl Acad Sci U S A 102(8):2754–2759
41. The fluorescence decay lifetime is a better and more quantitative measure of the Förster energy transfer as compared to the fluorescence intensity which is affected by the alignment of the pump-beam and the detection as well as the spectral response of the detector (Shim K, Kim S, Kim D, Oh-e M (2011) Fluorescence enhancement of dye-doped liquid crystal by dye-induced alignment effect. J Appl Phys 110(6): 063532)
42. Devaux A, Calzaferri G (2009) Manipulation of energy transfer processes in nanochannels. Int J Photoenerg 2009:9–17
43. Busby M, Devaux A, Blum C, Subramaniam V, Calzaferri G, Cola LD (2011) Interactions of perylene bisimide in the one-dimensional channels of zeolite L. J Phys Chem C 115 (13):5974–5988
44. Lutkouskaya K, Calzaferri G (2006) Transfer of electronic excitation energy between randomly mixed dye molecules in the channels of zeolite L. J Phys Chem B 110(11):5633–5638
45. Blumen A (1981) On the anisotropic energy transfer to random acceptors. J Chem Phys 74(12):6926–6933
46. van der Meer BW (2002) Kappa-squared: from nuisance to new sense. Rev Mol Biotechnol 82:181–196

47. Eisenthal KB, Siegel S (1964) Influence of resonance transfer on luminescence decay. J Chem Phys 41(3):652–655
48. Steinberg IZ (1968) Nonradiative energy transfer in systems in which rotatory brownian motion is frozen. J Chem Phys 48(6):2411–2413
49. Cao X, Tolbert RW, Mchale JL, Edwards WD (1998) Theoretical study of solvent effects on the intramolecular charge transfer of a hemicyanine dye. J Phys Chem A 102(17):2739–2748
50. Strehmel B, Seifert H, Rettig W (1997) Photophysical properties of fluorescence probes. 2: a model of multiple fluorescence for stilbazolium dyes studied by global analysis and quantum chemical calculations. J Phys Chem B 101(12):2232–2243
51. Shim T, Lee M, Kim S, Sung J, Rhee BK, Kim D, Kim H, Yoon KB (2004) Photoluminescence decay lifetime measurements of hemicyanine derivatives of different alkyl chain lengths. Mater Sci Eng C 24(1):83–85
52. Shim T, Lee M, Kim D, Ouchi Y (2008) Comparison of photophysical properties of the hemicyanine dyes in ionic and nonionic solvents. J Phys Chem B 112(7):1906–1912
53. Dulkeith E, Morteani AC, Niedereichholz T, Klar TA, Feldmann J, Levi SA, van Veggel FCJM, Reinhoudt DN, Möller M, Gittins DI (2002) Fluorescence quenching of dye molecules near gold nanoparticles: radiative and nonradiative effects. Phys Rev Lett 89 (20):203002–203005
54. Tomin VI (2009) Fluorescence quenching of photoreaction products in the excited singlet state. Russ J Phys Chem A 83(3):493–498